

## EVALUATION OF DEMENTIA-TYPE COGNITIVE DECLINE THROUGH 18F-FDG PET-CT QUANTIFICATION AND CORRELATIONS OF THE MMSE TEST WITH FUNCTIONAL IMAGING BIOMARKERS

Roxana Iacob<sup>1,2</sup>, O. Gherasim<sup>3</sup>, Irena Grierosu<sup>1,4\*</sup>, R. Stamate<sup>4</sup>,  
V. Ghizdovăț<sup>1</sup>, A. G. Naum<sup>1</sup>, Cipriana Ștefănescu<sup>1,4</sup>

“Grigore T. Popa” University of Medicine and Pharmacy, Iasi, Romania

1. Faculty of Medicine / Biophysics and Medical Physics Division

Regional Institute of Oncology, Iasi, Romania

2. Nuclear Medicine Department

Romanian Academy, Branch of Iași

3. “Gh. Zane” Institute of Economic and Social Researches

“Sf. Spiridon” County Clinical Emergency Hospital Iasi, Romania

4. Nuclear Medicine Department

\*Corresponding author. E-mail: irena.raileanu@umfiasi.ro

EVALUATION OF DEMENTIA-TYPE COGNITIVE DECLINE THROUGH 18F-FDG PET-CT QUANTIFICATION AND CORRELATIONS OF THE MMSE TEST WITH FUNCTIONAL IMAGING BIOMARKERS (Abstract): Recognition of the given moment when a mild cognitive impairment (MCI) converts to Alzheimer’s Disease (AD) represents a turning point in the assessment of the mental status rate of decline, but is still insufficiently systematically studied. Our aim was to contribute to the identification of the dementia irreversible starting point by cognitive assessment test Mini Mental State Examination (MMSE) and correlating it with the hybrid imaging technique positron emission tomography (PET) with fluor-18 fluorodeoxyglucose (<sup>18</sup>F-FDG) combined with localization computed tomography imaging (PET/CT), emphasizing that the method of quantification is crucial for patient evaluation and regression analysis can be helpful. **Materials and methods:** We studied 30 patients aged between 22 and 76 years presented during the assessment of their oncological pathologies. We evaluated their cognitive status by a MMSE test. All patients underwent a <sup>18</sup>F-FDG PET/CT examination, the image acquisition including the brain region. After specific image processing, characteristic regions of interest (ROIs) were identified, maximum and mean standardized values (SUVmax and SUVmean) were extracted. We computed correlations between 17 variables including: age, MMSE score value, glycemia, Administered Radiopharmaceutical Dose, Uptake Period, SUVmax and SUVmean for numerous ROIs as cerebral (SUVmaxCC) and cerebellar cortex (SUVmaxCc), posterior cingulate gyrus (SUVmaxPCG) and precuneus (SUVmaxP), as well as two SUV ratios: SUVRPCG and SUVRP. Calculation of mean, minimum, maximum and standard deviation have been made for each variable, and calculation of 4 regression functions (linear, exponential, power and logarithmic) and unique correlation analysis have been made for each pair of variables. **Results:** MMSE tests identified values of over 24, with an average of  $28.07 \pm 1.5DS$ , all patients examined having a normal cognitive status. SUVmaxPCG had values between 5.1 and 21.3 g/mL, with an average of  $13.36 \pm 3.77DS$ , SUVmeanPCG between 4 and 13.2 g/mL, average  $8.68 \pm 2.35DS$ , and SUVmaxP between 4.8 and 21 g/mL with an average of  $13.06 \pm 3.81DS$ ,

## Evaluation of dementia-type cognitive decline through <sup>18</sup>F-FDG PET-CT quantification and correlations of the MMSE test with functional imaging biomarkers

SUVmeanP between 4.1 and 14.1 g/mL with an average of  $9.93 \pm 2.73$ DS. From the 34 strong and very strong linear and exponential correlations identified between SUVs of the studied ROIs, 7 correlations have “extremely strong” values ( $R > 0.925$ ) including SUVs of AD cerebral specific ROIs. Also, there is a mean linear correlation between Age and MMSE score ( $R = 0.57$ ). **Conclusions:** Quantitative evaluation of <sup>18</sup>F-FDG PET-CT images for patients with neoplasia, found in a stage when an MCI can evolve simultaneously, could bring useful information for a possible early AD diagnostic and would be advisable in the precision medicine of the brain cognitive status evaluation. **Keywords:** COGNITIVE DECLINE, MILD COGNITIVE IMPAIRMENT (MCI), MMSE, PET/CT, IMAGING BIOMARKERS.

### INTRODUCTION

Alzheimer’s disease (AD) is the most common form of dementia, describing 60-70% of cases and affecting approximately 50 million of people worldwide, with an increasing incidence that could triple in the next 30 years, according to the World Health Organization in Guidelines for Risk Reduction of Cognitive Decline and Dementia (1). The adult process of neurogenesis is altered in the earliest stages of the disease, by progressive and irreversible loss of memory, of higher cerebral functions and later, of the self-help skill (2). Consistent with current guidelines, the diagnosis of AD involves clinical evidence of cognitive impairment, imagistic changes and accumulation of intracerebral biomarkers (3).

The brain has the highest avidity for glucose, consuming about 20% of the energy derived from its metabolism. But, in amnesic mild cognitive impairment (aMCI) and in AD, glucose metabolism is dramatically decreased, partly due to oxidative damage of enzymes involved in glycolysis, in tricarboxylic acid cycle and in adenosine triphosphate (ATP) biosynthesis, resulting synaptic dysfunction and neuronal death and thus the thinning of important areas of the cerebral cortex (4, 5, 6).

Neuroimaging, in particular hybrid functional and structural imaging, Single-photon

Emission Computed Tomography (SPECT) or Positron Emission Tomography (PET) with various radiotracers currently available, in combination with Computed Tomography (CT) or Magnetic Resonance Imaging (MRI), are complementary medical imaging techniques and essential tools for in vivo studies of neurocognitive disorders and especially of AD. While CT and specifically MRI provide cerebral structural information with a higher resolution (hippocampal volume reduction and loss of other structures from the temporal lobes, with neurodegeneration and tissue loss), PET imaging can provide metabolic and molecular information of the brain, with high sensitivity, by mapping the distribution of glucidic metabolism (decreased glucose avidity and neurodegeneration in the temporoparietal cortex, posterior cingulate gyrus and precuneus), of NFTs and  $\beta$ A deposits in the cerebral cortex, from the presymptomatic to the dementia stage (7, 8, 9, 10). The brain areas strictly involved in cognitive decline, the posterior cingulate cortex and the precuneus, are known to represent the first areas of metabolic alterations, that precede cognitive symptoms for patients with dementia and especially with AD.

aMCI is a clinical precursor of AD but only some patients at the respective stage will progress to irreversible AD. Recent

studies have shown that PET examination with the analog radiotracer of fluorine-18 fluorodeoxyglucose (18F-FDG PET) can detect prodromal AD and can highlight the progressive conversion of aMCI to AD with an accuracy of 89%, in a follow-up time of minimum 5 years. (11).

Histopathological changes such as amyloid  $\beta$  plaques ( $\beta$ A), neurofibrillary tangles of tau proteins (NFTs) and neuritic plaques precede symptomatology by more than a decade, during which treatment may be effective in slowing or even stopping the progression of the disease (12). Thus, in addition to serum biochemical markers (cerebral acetylcholinesterase, superoxide dismutase, glutathione peroxidase, catalase, total content of reduced glutathione, carbonyl protein and malondialdehyde and lactate dehydrogenase) and from cerebrospinal fluid (low or inadequate concentrations of  $\beta$ A fractions and increases in the concentration of hyperphosphorylated tau proteins) (6, 13), as well as the imaging markers mentioned above, other accessible and very effective methods, such as those of mathematical statistics, could help in the early diagnosis of the disease.

Assessing mental status and its rate of decline for a given population are still insufficiently studied issues. Cognitive assessment tests such as Mini-Mental State Examination (MMSE), involving the rapid assessment of time and space orientation skills, attention and calculation, comprehension, naming, repetition, memorization and reminder, reading, writing and drawing, are widely used methods for clinical monitoring of cognitive abilities in the elderly, but insufficient to assess the progression of dementia (14).

Although data from literature emphasize the importance of quantitative evaluation of

brain metabolism (4, 5, 6, 11, 12, 19, 20, 21, 22), the optimal method and the relationship between different methods that can be used in this regard have not yet been established and studies are still needed, each one bringing different information about the pathophysiology of AD development. In this context, this paper proposes a detailed study of data obtained for the cognitive and metabolic status of patients with potential cognitive decline to AD by the most used hybrid imaging technique PET/CT, qualitative and quantitative processing of functional metabolic images using specific software tools, their correlation with classic MMSE tests and statistical processing of obtained data. The novelty of the study is the combined analysis by specific methods and statistics of data obtained by MMSE and by 18F-FDG PET/CT, allowing correlations of special significance for patients with aMCI.

## MATERIALS AND METHODS

For this pilot study, we prospectively evaluated 30 patients from the Regional Institute of Oncology Iasi, Romania, known with various oncological pathologies and undergoing a PET/CT examination. The inclusion criteria included: adult patients hospitalized in the Regional Oncology Institute, Iasi, Romania, in the period June-July 2021, which have a recommendation for PET/CT scan, for the evaluation of the oncological disease. The exclusion criteria included: the patient does not want to participate and did not sign the informed consent; the patient has brain neoplasia (primary tumor or brain metastasis); the patient has a blood sugar level over 160 mg/dL even after a correction attempt, represented by the intravenous administration of 500 mL physiological serum.

## **Evaluation of dementia-type cognitive decline through $^{18}\text{F}$ -FDG PET-CT quantification and correlations of the MMSE test with functional imaging biomarkers**

All imaging protocols were approved by an internal review board. Prior to participation in this study, signed informed consent for PET/CT examination and for data processing was obtained from all participant patients. The study was approved by the Ethical Committee of "Grigore T. Popa" U.M.Ph. Iasi Doctoral School, being part of the doctoral studies of the first author.

After performing an anamnesis specific to the basic pathology of each patient, we performed a standardized cognitive impairment assessment by applying the MMSE test, to evaluate the skills of orientation, attention and calculation, understanding and memory.

Each patient underwent a rigorous and specific preparation for PET/CT examination with an analog glucose radiotracer. Patients with glycemic levels above 160 mg/dL received a 500 mL saline infusion before injecting the radiotracer, normalizing glycemia according to the EANM recommendations for clinical trials (16).

### **Acquisition of imaging data and reconstruction of images**

In the context of pre-existing oncological pathologies evaluation, all patients needed to perform a  $^{18}\text{F}$ -FDG PET/CT examination, the acquisition of images including the brain region. The examination was performed using a fully integrated 3D PET/CT Discovery 710 scanner from General Electric and consisted in a full body acquisition CT scout and in two vertex-thigh (10 beds) or vertex-hallux (17 beds) acquisitions, with an acquisition speed of 2 minutes per bed, depending on the existing oncological pathology: one low-dose CT for localization and attenuation correction and another PET.

The dose of radiotracer administered

and the uptake period from the time of administration to image acquisition have met the European Association of Nuclear Medicine required standards, the dose ranging from 235 to 592 MBq, with an average of  $374.27 \pm 55.7$  MBq, depending on individual body weight, with the uptake period of 44 to 76 minutes, and an average of  $55.7 \pm 9.5$  minutes (3, 15, 16).

The specific processing consisted in the use of basic reconstruction algorithms of OSEM type (ordered-subsets expectation-maximization algorithm) and secondary algorithms of NAC type (non-attenuation correction) and TOF AC type (time-of-flight attenuation correction). The study of images in two dimensions (2D), in three different incidences (axial, coronal and sagittal), as well as in three dimensions (3D, maximum intensity projections or MIP) allowed the analysis of four sets of images per patient (axial, coronal, sagittal and MIP), i.e. the analysis of a total of 120 sets of images.

After specific processing of the acquired images, characteristic regions of interest (ROIs) were identified and plotted on surfaces of 20 mm diameter, both the maximum and the mean standardized uptake values (SUVmax and SUVmean) being subsequently extracted from the following general regions: descending aorta (Ao) corresponding to circulating metabolic activity and bladder or the most intense area of extracerebral glucidic uptake (B), as well as specific regions for functional imaging assessment of dementia: cerebral cortex (CC), cerebellar cortex (Cc), posterior cingulate gyrus (PCG) and precuneus (P). SUVmax and SUVmean values of general and specific ROIs plotted on the two-dimensional images were collected for each patient and statistically analyzed (fig. 1).

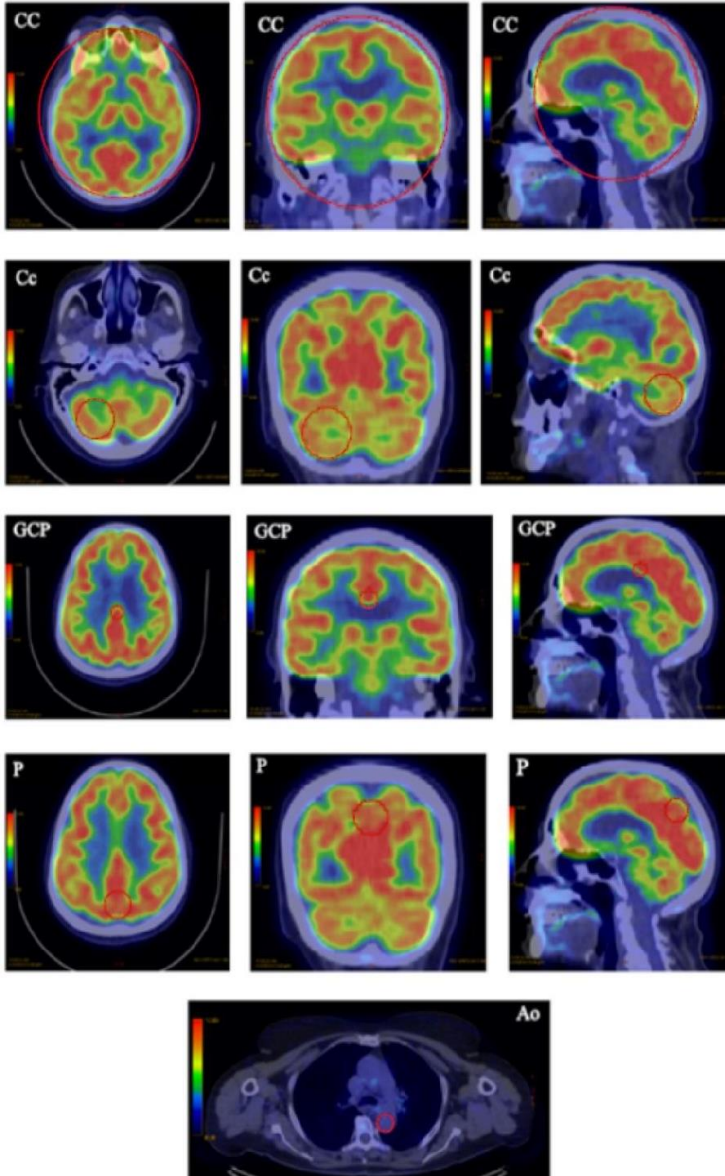


**Fig. 1.**  $^{18}\text{F}$ -FDG PET/CT images axial, coronal and sagittal sections. UV values were collected by delimiting ROIs (dark red circles) in the (CC) Cerebral Cortex, (Cc) Cerebellar cortex, (PCG) Posterior Cingulate Gyrus, (P) Precuneus and (Ao) Descending Aorta

**Numerical data analysis**

All numerical data used, 17 variables marked V1-V17, are listed in the first table. Statistical processing included the clas-

sical calculation of the following values: mean, minimum, maximum and standard deviation (*SD*). After that, 4 regression functions are calculated (linear, exponen-

**Evaluation of dementia-type cognitive decline through 18F-FDG PET-CT quantification and correlations of the MMSE test with functional imaging biomarkers**

tial, power and logarithmic) for each pair of variables, as described in previous articles (17, 18). The formulas can be seen in the second table. For each type of correlation, we calculated the correlation coefficient (R) or the ratio between the variable's

covariance and the product of their SDs

For the variables V1 - V7, V8 or V14, the unique correlation analysis allows the value identification of one variable, knowing only the value of another variable and applying the unique correlation formula.

TABLE I.

**List of variables studied for each patient**

V1	V2	V3	V4	V5	V6	V7	V8	V9
Age (years old)	MMSE Score	Glycemia (mg/dL)	Administered Dose (MBq)	Uptake Period (minutes)	SUVmaxAo (g/mL)	SUVmaxB (g/mL)	SUVmaxCC (g/mL)	SUVmaxCc (g/mL)
V10	V11	V12	V13	V14	V15	V16	V17	
SUVmaxPCG (g/mL)	SUV maxP (g/mL)	SUVRPCG	SUVRP	SUVmeanCC (g/mL)	SUVmeanCc (g/mL)	SUVmeanPCG (g/mL)	SUVmeanP (g/mL)	

Age, MMSE Score, Glycemia, Administered Radiopharmaceutical Dose, Uptake Period from injection to examination moment, SUVmax and SUVmean values in (CC) Cerebral Cortex, (Cc) Cerebellar cortex, (PCG) Posterior Cingulate Gyrus, (P) Precuneus, (Ao) Descending Aorta and (B) Bladder, as well as the SUVR for Posterior Cingulate Gyrus represented by  $SUVRPCG = SUVmaxPCG / SUVmaxCc$  and for Precuneus represented by  $SUVRP = SUVmaxP / SUVmaxCc$ .

TABLE II.

**Variables and correlations calculated**

Operation	Formula	Explanations
Linear Correlation	$Y = a \cdot x + b$	x - the independent variable, Y - the calculated variable, a, b - known, constant numbers in the formula, e - the mathematical constant of the exponential ~ 2,71828
Exponential Correlation	$Y = e^{a \cdot x + b}$	
Logarithmic Correlation	$Y = a \cdot \ln x + b$	
Power Correlation	$Y = b \cdot x$ (weak for all correlations)	
Correlation coefficient (R)	$R = \frac{\sum_{i=1}^n (x_i - \bar{x})(y_i - \bar{y})}{\sqrt{\sum_{i=1}^n (x_i - \bar{x})^2} \sqrt{\sum_{i=1}^n (y_i - \bar{y})^2}}$	x = x <sub>1</sub> , x <sub>2</sub> , ...x <sub>i</sub> , ...x <sub>n</sub> and y=y <sub>1</sub> , y <sub>2</sub> , ...y <sub>i</sub> , ...y <sub>n</sub> - the values of the x and y variables, $\bar{x}$ and $\bar{y}$ - the averages of the respective variables, R - a number between -1 and 1, indicates the strength of the connection between the two variables (close to 1 -strong bond, 0.5 - average correlation, 0.2 - weak correlation, ≤ 0.1 - lack of correlation).

**RESULTS**

The 30 studied patients had between 22 and 76 years old, with a balanced male / female ratio of 1.14 (16 men and 14 women). The mean age was  $54.03 \pm 16.76$  SD, divided into age groups: 6 young adults between 20-40 years old, 10 adults between 41-60 years old, 13 middle-old people between 61-75 years old, 1 old man over 76 years old. None of the subjects had an associated cerebral malignant pathology.

The patients group studied had a mean glycemia (V3) of  $99.03 \text{ mg/dL} \pm 21.96$  SD, with a minimum of 64 mg/dL and a maximum of 179.82 mg/dL.

MMSE tests identified values between 24.4 and 30 and an average of  $28.07 \pm 1.5$ DS, all patients examined having a normal cognitive status. The distribution of MMSE evaluation results by age groups is presented in the second figure.

From the acquired imaging data, *SU-*

*Vmax<sub>PCG</sub>(V10)* had values between 5.1 and 21.3 g/mL, with an average of  $13.36 \pm 3.77$  SD, *SUVmean<sub>PCG</sub>(V16)* between 4 and 14 g/mL, an average of  $8.68 \pm 2.35$  SD, and *SUVmax<sub>P</sub>(V11)* between 4.8 and 21 g/mL with an average of  $13.06 \pm 3.81$  SD, respectively *SUVmean<sub>P</sub>(V17)* between 4.1 and 14.1 g/mL, with an average of  $9.93 \pm 2.73$  SD.

The mean, minimum, maximum, and SD values for all variables are listed in table III.

Linear, exponential, power and logarithmic regression functions were calculated and the strongest was recorded. As example, for the correlation *SUVmean<sub>P</sub>-SUVmean<sub>PCG</sub> (V17-V16)* we calculated the 4 regression functions, the strongest being the linear one ( $R=0.900$ ), where x is the independent variable V16 and Y(x) is the calculated variable V17:  $Y_{((x))} = 1.044 \cdot x + 0.860$ .

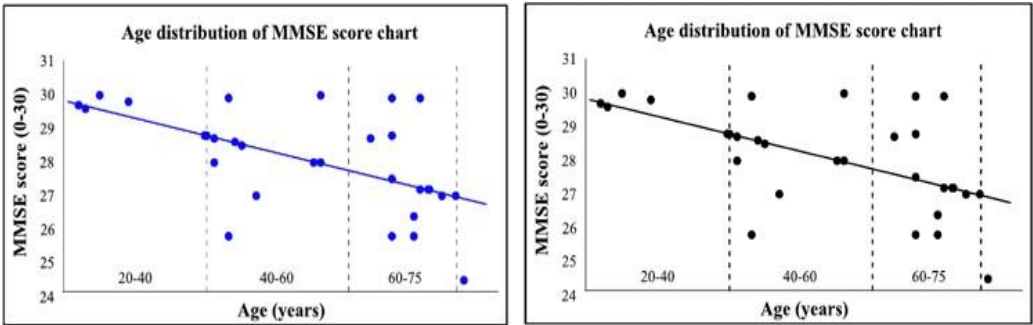


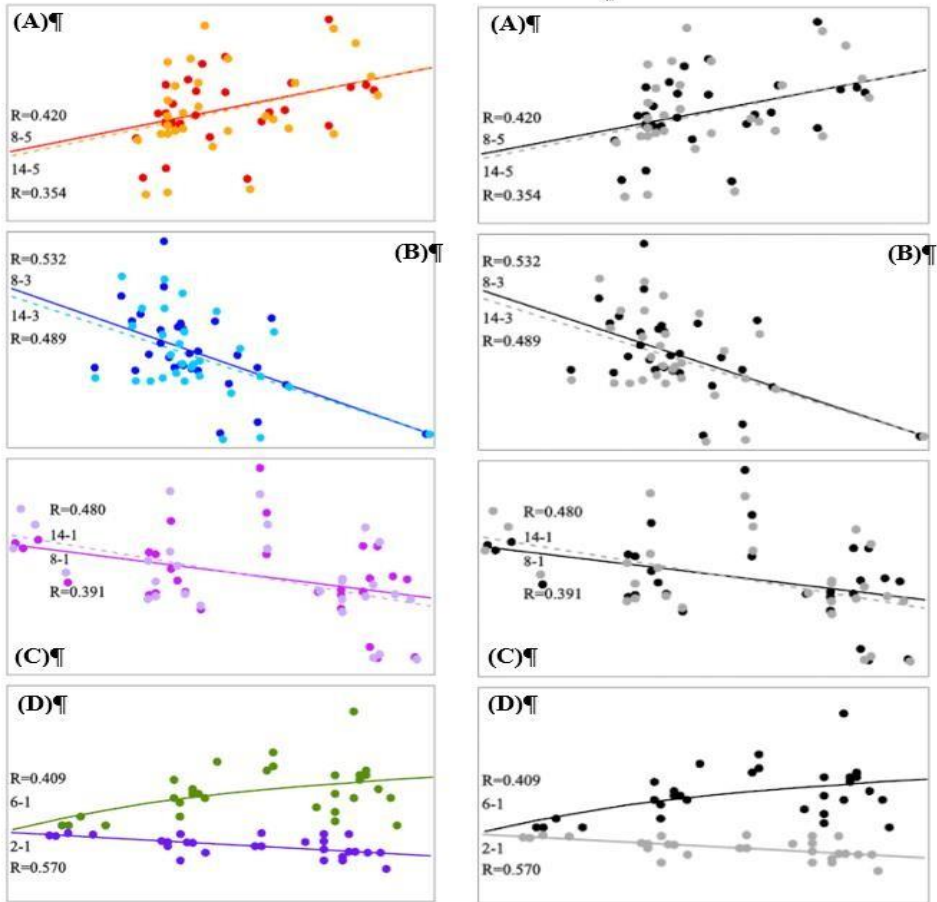
Fig. 2. Age distribution of MMSE score chart.

TABLE III.

**Statistical calculation of mean, minimum, maximum and standard deviation values**

	V1	V2	V3	V4	V5	V6	V7	V8	V9	V10	V11	V12	V13	V14	V15	V16	V17
<b>Mean</b>	54.03	28.07	99.03	374.3	55.70	2.64	31.98	15.31	11.40	13.36	13.06	1.16	1.13	5.52	7.46	8.68	9.93
<b>SD</b>	16.76	1.50	21.96	72.37	9.51	0.56	22.67	4.49	2.45	3.77	3.81	0.14	0.18	1.44	1.95	2.35	2.73
<b>Min</b>	22.00	24.50	64.0	235.8	44.0	1.90	5.90	6.20	5.60	5.10	4.80	0.91	0.81	2.7	3.8	4.0	4.1
<b>Max</b>	76.00	30.00	179.8	592.2	76.00	4.40	103.9	27.20	16.70	21.30	21.00	1.58	1.54	8.3	12.5	14.0	14.1

**Evaluation of dementia-type cognitive decline through 18F-FDG PET-CT quantification and correlations of the MMSE test with functional imaging biomarkers**



**Fig. 3.** Significant regression functions ( $R > 0.350$ ) by unique correlation analysis. Correlations between (A) Uptake Period (5) and SUVmaxCC (8) or SUVmeanCC (14); (B) Glycemia (3) and SUVmaxCC (8) or SUVmeanCC (14); (C) Age (1) and SUVmaxCC (8) or SUVmeanCC (14); (D) Age (1) and MMSE (2) or SUVmaxAo (6)

No correlation was observed between the administered dose and any other variable, the doses being those recommended by international guidelines.

Slightly above average reverse correlations ( $R > 0.5$ ) were found between glycemia and cerebral SUVs, and a slightly higher between glycemia above 120 mg/dL and corresponding SUVs. The same kind of correlation was found between blood glucose

and SUVs in specific ROIs SUVmax/meanGCP and SUVmax/meanP, denoting the dependence between brain glucose metabolism and plasma blood glucose.

Using only the function with the highest regression coefficient  $R$ , we obtained 34 “strong” correlations ( $R > 0.75$ ), of which 16 “very strong” ( $R \geq 0.9$ ), and 3 correlations presenting “assimilable” value slopes ( $R > 0.945$ ).



From these 34 strong and very strong linear and exponential correlations identified between SUVs of the studied ROIs, 7 correlations have “extremely strong” R values ( $R > 0.925$ ) including SUVs of AD cerebral specific ROIs. Four sets of variables have an obvious correlation by the calculation formula of the maximum and average SUVs: SUV<sub>meanP</sub>–SUV<sub>maxP</sub> (V17-V11), SUV<sub>meanPCG</sub>–SUV<sub>maxPCG</sub> (V16-V10), SUV<sub>meanCc</sub>–SUV<sub>maxCc</sub> (V15-V9) and SUV<sub>meanCC</sub>–SUV<sub>maxCC</sub> (V14-V8). The correlation between SUV<sub>meanP</sub>–SUV<sub>maxPCG</sub> (V17-V10) is also partially related to the calculation formula. Four other sets: SUV<sub>maxPCG</sub>–SUV<sub>maxCC</sub> (V10-V8) ( $R = 0.946$ ), SUV<sub>maxP</sub>–SUV<sub>maxPCG</sub> (V11-V10) ( $R = 0.939$ ), SUV<sub>maxP</sub>–SUV<sub>maxCC</sub> (V11-V8) ( $R = 0.915$ ), SUV<sub>maxPCG</sub>–SUV<sub>maxCc</sub> (V15-V10) ( $R = 0.914$ ) and their SUV<sub>mean</sub> correspondents are of particular significance, denoting the anatomic-pathological connection between these cerebral regions.

From the unique correlation analysis, we also withhold the average and slightly below average linear correlations ( $R > 0.350$ ) between SUV<sub>maxCC</sub> (V8) or SUV<sub>meanCC</sub> (V14) and Uptake Period (V5), Glycemia (V3) respective Age (V1). The logarithmic correlation between SUV<sub>maxAo</sub> (V6) and Age (V1) and the linear correlation between MMSE score (V2) and Age (V1) have also statistical and medical significance (fig. 3).

Other correlations between the MMSE score and other variables didn't bring relevant information.

Further, the values of the other 16 dependent variables were obtained from the values of the independent variable V8, with regression functions (tab. IV).

Other correlations between different

components of MMSE test and other variables did not brought significant data.

Several <sup>18</sup>F-FDG PET image analysis methods have been used to predict and detect aMCI conversion to irreversible AD, from qualitative, visual analysis to different quantitative methods: quantitative analysis by traditional and automated methods of deep learning-based algorithms, starting with Minoshima S *et al.* in 1995 (19) until these last years, with the work of De Carli F *et al.* in 2019 based on a Support-Vector Machine (20) or Pan X *et al.* in 2021 with their Multi-View Separable Pyramid Network (21). Voxel wise Cox regression based in <sup>18</sup>F-FDG PET data for prediction of aMCI conversion to AD was described by Sorensen *et al.* in 2019 (22) and Duan J *et al.* proposed BLADNet in 2023 (23). All these methods, although in different ways, have the same goal as our studies, emphasizing the importance of quantitative image evaluation. Being based also in a regression formula, Sorensen's study is the closest to our try to underline the crucial importance of quantification methods to identify the dementia irreversible starting point by regression analysis.

Our studies of quantitative evaluation of particular cerebral ROIs bring some contribution compared to qualitative evaluation. Our data demonstrated significant correlations between SUVs of specific cerebral ROIs and weak correlations between MMSE score and SUVs in the specific ROIs where modifications appear in different dementias, anatomic-pathological connections between these specific ROIs being undeniable.

The dependence between brain metabolism and glycemic levels shown in our data analysis with slightly above average reverse correlations ( $R > 0.5$ ) is supported by

**Evaluation of dementia-type cognitive decline through 18F-FDG PET-CT quantification and correlations of the MMSE test with functional imaging biomarkers**

literature (24). The total cerebral SUV and specific cerebral SUVs are values affected by glycemia, subjects with higher glucose levels presenting lower SUVmax/mean.

TABLE IV.  
Single correlation regression functions for the independent variable SUVmaxCC (V8) and its degree of correlation

Weak (& v.w.)	$V2(V8) = 0.486 \cdot V8 + 20.651$	$V4(V8) = -200 \cdot V8 + 191.6$	
	$V6(V8) = 0.687 \cdot \ln(-9.524 \cdot V8 + 199.657) - 0.060$		$V7(V8) = -4.566 \cdot V8 + 101.826$
Medium	$V1(V8) = -9.524 \cdot V8 + 199.657$	$V3(V8) = -9.174 \cdot V8 + 239.165$	$V5(V8) = 5,051 \cdot V8 - 21.576$
Strong correlations	$V9(V8) = 0.505 \cdot V8 + 3.664$	$V10(V8) = 0.796 \cdot V8 + 1.176$	$V11(V8) = 0.755 \cdot V8 + 1.516$
	$\frac{0.796 \cdot V_8 + 1.176}{V12(V8) = 0.505 \cdot V + 3.6648}$	$\frac{0.755 \cdot V_8 + 1.516}{V13(V8) = 0.505 \cdot V + 3.6648}$	$V14(V8) = 0.298 \cdot V8 + 0.958$
	$V15(V) = e^{0.0535 \cdot V8 + 1.1578}$	$V16(V8) = 0.479 \cdot V8 + 1.342$	$V17(V8) = 0.522 \cdot V8 + 1.940$

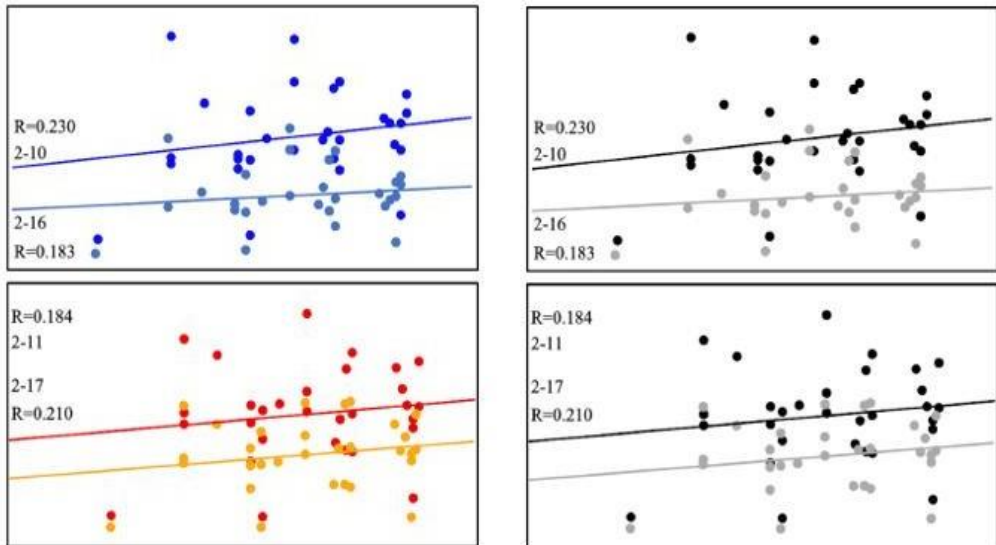


**Fig. 4.** Correlations between MMSE and AD specific cerebral SUVs

**DISCUSSION**

We observed that strictly following the protocols recommended by international guidelines, in terms of administered radio-pharmaceutical dose, image acquisition protocol, and radiotracer uptake period, patient’s blood glucose level before exami-

nation, is an essential step (16, 24).

It is also very important to make a judicious choice of the ROIs used for these correlations, allowing future development of some automatic correlations. It is important, also, that the patients do not have brain neoplasia diagnosis. Neurological functions

are not influenced by malignant pathology as long as patients do not have brain neoplasia, including cerebral metastases.

Different correlations between brain areas with important etiopathogenic involvement for AD suggest the usefulness of introducing an index of MCI metabolic visualization in order to identify early dementia. To obtain such an index between specific ROIs requires prospective studies on groups of patients with varying degrees of MCI and AD. Because subjects may perform  $^{18}\text{F}$ -FDG PET repeatedly, meantime a MCI process may evolve concomitantly with the malignant pathology, this possibility supporting the usefulness of brain additional quantitative analyzes by introducing such index of MCI status.

Our studies are limited partly by the number of subjects and by the nonspecific pathologies of our patients.

We intend to extend this pilot study to a larger number of patients. Given the neoplasia patients indication for PET-CT images, a limitation of our study could be the uptake period that was established in relation to malignant pathology, also.

Other studies could be developed by improving AD neuroimaging database and by a more complex prospective predictive

methodology. A direction would be the elaboration of forecasting software for aMCI to irreversible AD conversion, including multiple dependence correlation formulas with the most powerful connections between variables.

Considering the fact that many patients may be in the borderline period, still socially active, early diagnosis of predementia MCI is useful for limiting economic losses by delaying the onset of AD, thus achieving an MCI and AD precision medicine.

## CONCLUSIONS

Even for the identification of a dementia irreversible starting point studies on a greater number of patients are still necessary, our results support the conclusion that the quantitative evaluation of  $^{18}\text{F}$ -FDG PET-CT images for cancer patients found in a stage when an MCI can evolve simultaneously would be advisable and could bring useful information for the early onset diagnostic in the precision medicine of the brain process of cognitive loss.

## CONFLICT OF INTEREST AND FUNDING

The authors declare that there is no conflict of interest and they received no funding.

## REFERENCES

1. World Health Organization. Risk Reduction of Cognitive Decline and Dementia: *WHO Guidelines*. Geneva, 2019.
2. Jack CR Jr, Bennett DA, Blennow K, *et al.* NIA-AA Research Framework: Toward a biological definition of Alzheimer's disease. *Alzheimers Dement* 2018; 14(4): 535-562.
3. Nobili F, Arbizu J, Bouwman F, *et al.* EANM-EAN Task Force for the Prescription of FDG-PET for Dementing Neurodegenerative Disorders. European Association of Nuclear Medicine and European Academy of Neurology recommendations for the use of brain (18) F-fluorodeoxyglucose positron emission tomography in neurodegenerative cognitive impairment and dementia: Delphi consensus. *Eur J Neurol* 2018; 25(10): 1201-1217.
4. Mergenthaler P, Lindauer U, Dienel G, Meisel A. Sugar for the brain: the role of glucose in physiological and pathological brain function. *Trends Neurosci* 2013; 36(10): 587-597.

## Evaluation of dementia-type cognitive decline through 18F-FDG PET-CT quantification and correlations of the MMSE test with functional imaging biomarkers

5. Butterfield DA, Halliwell B. Oxidative stress, dysfunctional glucose metabolism and Alzheimer disease. *Nat Rev Neurosci* 2019; 20(3): 148-160.
6. Frisoni GB, Boccardi M, Barkhof F, *et al.* Strategic roadmap for an early diagnosis of Alzheimer's disease based on biomarkers. *Lancet Neurol* 2017; 16(8): 661-676.
7. Mainta IC, Perani D, Delattre BM, *et al.* FDG PET/MR Imaging in Major Neurocognitive Disorders. *Curr Alzheimer Res* 2017; 14(2): 186-197.
8. Shimizu S, Hirose D, Hatanaka H, *et al.* Role of Neuroimaging as a Biomarker for Neurodegenerative Diseases. *Front Neurol* 2018; 9: 265.
9. Sanchez-Catasus CA, Stormezand GN, van Laar PJ, De Deyn PP, Sanchez MA, Dierckx RA. FDG-PET for Prediction of AD Dementia in Mild Cognitive Impairment. A Review of the State of the Art with Particular Emphasis on the Comparison with Other Neuroimaging Modalities (MRI and Perfusion SPECT). *Curr Alzheimer Res* 2017; 14(2):127-142.
10. Ricci M, Cimini A, Chiaravalloti A, Filippi L, Schillaci O. Positron Emission Tomography (PET) and Neuroimaging in the Personalized Approach to Neuro-degenerative Causes of Dementia. *Int J Mol Sci* 2020; 21(20): 7481.
11. Pagani M, Nobili F, Morbelli S, *et al.* Early identification of MCI converting to AD: a DG PET study. *Eur J Nucl Med Mol Imaging* 2017; 44: 2042-2052.
12. Fernández-Blázquez MA, Ávila-Villanueva M, Maestú F, Medina M. Specific Features of Subjective Cognitive Decline Predict Faster Conversion to Mild Cognitive Impairment. *J Alzheimers Dis* 2016; 52(1): 271-281.
13. Qu Z, Zhang J, Yang H, *et al.* Protective effect of tetrahydropalmatine against d-galactose induced memory impairment in rat. *Physiol Behav* 2016; 154: 114-125.
14. Creavin S, Wisniewski S, Noel-Storr A, *et al.* Mini-Mental State Examination (MMSE) for the Detection of Dementia in Clinically Unevaluated People Aged 65 and Over in Community and Primary Care Populations. *Cochrane Database Syst Rev* 2016; (1): CD011145.
15. Varrone A, Asenbaum S, Vander Borcht T, *et al.* EANM procedure guidelines for PET brain imaging using (18F)FDG, version 2. *Eur J Nucl Med Mol Imaging* 2009; 36(12): 2103-2110.
16. Schoen M, Braun T, Manava P, Ludwigs S, Lell M. Influence of scan time point and volume of intravenous contrast administration on blood-pool and liver SUVmax and SUVmean in (18F) FDG PET/CT. *Nuklearmedizin* 2018; 57(2):50-55.
17. Iacob R, Ștefănescu C. Cognitive decline status on highly educated persons – a pilot correlational study. In: *Identity and Dialogue in the Era of Globalization*, Iulian Boldea I, Sigmirean C (ed.) Târgu-Mureș Arhipelag XXI Press, 2019, 21-31.
18. Gherasim O, Iacob R. Fuzzy assessments for economic indicators. In *Romanian Rural Tourism in International Context. Present and Prospects*. Iași: Performantica 2017; XLIII (IV): 216-221.
19. Minoshima S, Frey KA, Koeppe RA, Foster NL, Kuhl DE. A diagnostic approach in Alzheimer's disease using threedimensional stereotactic surface projections of fluorine-18-FDG PET. *J Nucl Med* 1995; 36(7): 1238-1248.
20. De Carli F, Nobili F, Pagani M, *et al.* Alzheimer's Disease Neuroimaging Initiative. Accuracy and generalization capability of an automatic method for the detection of typical brain hypometabolism in prodromal Alzheimer disease. *Eur J Nucl Med Mol Imaging* 2019; 46(2): 334-347.
21. Pan X, Phan T-L, Adel M, *et al.* Multi-View Separable Pyramid Network for AD Prediction at MCI Stage by 18 FFDG Brain PET Imaging. *IEEE Trans Med Imaging* 2021; 40(1): 81-92.
22. Sörensen A, Blazhenets G, Rucker G, Schiller F, Meyer PT, Frings L. Alzheimer's Disease Neuroimaging Initiative. Prognosis of conversion of mild cognitive impairment to Alzheimer's dementia by voxel-wise Cox regression based on FDG PET data. *Neuroimage Clin* 2019; 21: 101637.
23. Duan J, Liu Y, Wu H, Wang J, Chen L, Chen CLP. Broad learning for early diagnosis of Alzheimer's disease using FDG-PET of the brain. *Front Neurosci* 2023; 17: 1137567.
24. Sprinz C, Altmayer S, Zanon M, *et al.* Effects of blood glucose level on 18F-FDG uptake for PET/CT in normal organs: A systematic review. *PLoS One* 2018; 13(2): e0193140.